Flexural Capacity of Fire-Damaged Prestressed Concrete Box Beams

PUBLICATION NO. FHWA-HRT-07-024

FEBRUARY 2007

U.S. Department of Transportation
Federal Highway Administration

Research, Development, and Technology
Turner-Fairbank Highway Research Center
6300 Georgetown Pike
McLean, VA 22101-2296

FOREWORD

The Federal Highway Administration, at the request of the Connecticut Department of Transportation, has investigated the flexural capacity of a set of prestressed concrete adjacent box beams that were damaged in a fire. The U.S. Route 7 bridge over the Norwalk River near Ridgefield, CT was damaged when a gasoline tanker crashed and caught fire on the bridge. During the replacement of the superstructure of this bridge, four beams were saved and transported to the Turner-Fairbank Highway Research Center. Full-scale structural tests were completed on the beams to determine their flexural behavior through ultimate failure. Additional visual and petrographic examinations were also completed. In summary, the investigation found that the flexural capacity of the beams had not been degraded significantly as compared to their anticipated capacity; however, their long-term durability may have been degraded by the fire. This report presents the results of this experimental investigation.

Gary L. Henderson
Director, Office of Infrastructure
Research and Development

Technical Report Documentation Page

1. Report No. FHWA-HRT-07-024	2.	3. Recipients Accession No.	
4. Title and Subtitle Flexural Capacity of Fire-Damaged Prestressed Concrete Box Beams		5. Report Date February 2007	
		6.	
7. Author(s) Benjamin A. Graybeal		8. Performing Organization Report No.	
9. Performing Organization Name and Address PSI, Inc. 2930 Eskridge Road Fairfax, VA 22031		10. Project/Task/Work Unit No.	
		11. Contract (C) or Grant (G) No.	
12. Sponsoring Organization Name and Address Office of Research and Technology Service Federal Highway Administration 6300 Georgetown Pike McLean, VA 22101-2296		13. Type of Report and Period Covered Final Report, December 2005 – July 2006	
		14. Sponsoring Agency Code	
15. Supplementary Notes Additional FHWA Contacts—William Wright, Contract Officer's Technical Representative			
16. Abstract (Limit: 200 words) A gasoline tanker truck fire caused significant damage to an adjacent member box-beam bridge in southwestern Connecticut. It was unclear whether the type of damage that these box beams experienced was sufficient to critically impair the structure's ability to serve its intended purpose. Four of the beams were removed from the bridge and were loaded in flexure to failure. These tests indicated that each of the beams retained sufficient flexural capacity to resist a 1,572 kilonewton-meter (kN-m) (1,160 kip-feet (kip-ft)) moment prior to ultimate flexural failure. This value is greater than the rated ultimate flexural capacity of each beam. As such, it seems that these beams had sufficient remaining flexural capacity to serve their intended purpose in the immediate aftermath of the fire. The long-term viability of these beams is more questionable. The visual and petrographic examinations indicated that the damage to the bottom flange concrete was sufficient to allow pathways through the concrete to the depth of the bottom strands. Therefore, it is possible that fire may have acted to allow for the accelerated deterioration of the superstructure and thus decreased the long-term flexural capacity of the bridge.			
17. Document Analysis/Descriptors Fire Damage, Prestressed Concrete, Adjacent Box Beam Bridge, Flexural Capacity		18. Availability Statement	
19. Security Class (this report) Unclassified	20. Security Class (this page) Unclassified	21. No. of Pages 35	22. Price

Form DOT F 1700.7 (8-72) Reproduction of completed page authorized.

SI* (MODERN METRIC) CONVERSION FACTORS

APPROXIMATE CONVERSIONS TO SI UNITS

Symbol	When You Know	Multiply By	To Find	Symbol
		LENGTH		
in	inches	25.4	millimeters	mm
ft	feet	0.305	meters	m
yd	yards	0.914	meters	m
mi	miles	1.61	kilometers	km
		AREA		
in^2	square inches	645.2	square millimeters	mm^2
ft^2	square feet	0.093	square meters	m^2
yd^2	square yard	0.836	square meters	m^2
ac	acres	0.405	hectares	ha
mi^2	square miles	2.59	square kilometers	km^2
		VOLUME		
fl oz	fluid ounces	29.57	milliliters	mL
gal	gallons	3.785	liters	L
ft^3	cubic feet	0.028	cubic meters	m^3
yd^3	cubic yards	0.765	cubic meters	m^3
		NOTE: volumes greater than 1000 L shall be shown in m^3		
		MASS		
oz	ounces	28.35	grams	g
lb	pounds	0.454	kilograms	kg
T	short tons (2000 lb)	0.907	megagrams (or "metric ton")	Mg (or "t")
		TEMPERATURE (exact degrees)		
^oF	Fahrenheit	5 (F-32)/9 or (F-32)/1.8	Celsius	^oC
		ILLUMINATION		
fc	foot-candles	10.76	lux	lx
fl	foot-Lamberts	3.426	$candela/m^2$	cd/m^2
		FORCE and PRESSURE or STRESS		
lbf	poundforce	4.45	newtons	N
lbf/in^2	poundforce per square inch	6.89	kilopascals	kPa

APPROXIMATE CONVERSIONS FROM SI UNITS

Symbol	When You Know	Multiply By	To Find	Symbol
		LENGTH		
mm	millimeters	0.039	inches	in
m	meters	3.28	feet	ft
m	meters	1.09	yards	yd
km	kilometers	0.621	miles	mi
		AREA		
mm^2	square millimeters	0.0016	square inches	in^2
m^2	square meters	10.764	square feet	ft^2
m^2	square meters	1.195	square yards	yd^2
ha	hectares	2.47	acres	ac
km^2	square kilometers	0.386	square miles	mi^2
		VOLUME		
mL	milliliters	0.034	fluid ounces	fl oz
L	liters	0.264	gallons	gal
m^3	cubic meters	35.314	cubic feet	ft^3
m^3	cubic meters	1.307	cubic yards	yd^3
		MASS		
g	grams	0.035	ounces	oz
kg	kilograms	2.202	pounds	lb
Mg (or "t")	megagrams (or "metric ton")	1.103	short tons (2000 lb)	T
		TEMPERATURE (exact degrees)		
^oC	Celsius	1.8C+32	Fahrenheit	^oF
		ILLUMINATION		
lx	lux	0.0929	foot-candles	fc
cd/m^2	$candela/m^2$	0.2919	foot-Lamberts	fl
		FORCE and PRESSURE or STRESS		
N	newtons	0.225	poundforce	lbf
kPa	kilopascals	0.145	poundforce per square inch	lbf/in^2

*SI is the symbol for the International System of Units. Appropriate rounding should be made to comply with Section 4 of ASTM E380.
(Revised March 2003)

TABLE OF CONTENTS

LIST OF FIGURES

LIST OF TABLES

CHAPTER 1. INTRODUCTION

INTRODUCTION

A fiery incident involving a gasoline tanker truck caused significant damage to an adjacent member box-beam bridge in southwestern Connecticut. Although the Connecticut Department of Transportation (ConnDOT) decided to replace the superstructure of the bridge, they were also interested in determining whether the type of damage that these box beams experienced was sufficient to critically impair the structure's ability to serve its intended purpose. To reach this end, ConnDOT coordinated with the Federal Highway Administration's (FHWA) Turner-Fairbank Highway Research Center to investigate the remaining flexural capacity of the beams in the bridge. Four of the beams were tested to failure and the results are reported herein.

INCIDENT

On the afternoon of July 12, 2005, a gasoline tanker truck traveling north on U.S. Route 7 near Ridgefield, CT overturned and exploded. The truck came to rest on the east side of the northbound shoulder of the Route 7 bridge over the Norwalk River. The 30,300 liters (8,000 gallons) of burning fuel flowed over the bridge and into the river below. As evidenced by the melting and possible vaporization of the aluminum that was originally part of the tanker truck, the temperature in the immediate vicinity of the truck could have been over 2,467 °C (4,472 °F). Figure 1 shows the remains of the tanker truck on the bridge after the fire.

Photo Credit: Ronald D. Jantzen

Figure 1. Photo. Remains of tanker truck after fire.

BRIDGE STRUCTURE

The U.S. Route 7 bridge over the Norwalk River is a single span bridge composed of 15 prestressed adjacent box beams. The bridge carries two lanes of traffic and two shoulder lanes, with a relatively shallow clearance over the river. The bridge was constructed in 1957 and spans 14.6 meters (m) (48 feet (ft)). The beams were 0.91-m (36-inches) wide and 0.64-m (25-inches) deep. The beams were topped by a waterproofing membrane and a 160-millimeter (mm)- (6.25-inch-) thick bituminous concrete overlay.

The most recent rating of this bridge was completed in 1999. This load factor analysis was conducted on a representative interior member of the bridge. It concluded that these beams have an inventory rating of 1.33 and an operating rating of 2.23 under HS20 live loading with shear capacity governing in both cases. This analysis also indicated that the ultimate moment capacity of each beam is 1407 kilonewton-meter (kN-m) (1038 kip-ft), corresponding to an inventory rating of 1.42 and an operating rating of 2.63.

POST-INCIDENT BRIDGE CONDITION EVALUATION

Visual examination of the bridge structure immediately after the fire found that scaling of the concrete surface had occurred on the bottom flanges of all 15 beams as well as on the exterior faces of the fascia beams. The bridge fascia is shown in Figure 2. The bituminous concrete overlay in the immediate vicinity of the tanker truck was in poor condition, but the membrane was intact. As nondestructive means were not available to quantify the integrity of the prestressing strands, ConnDOT decided to replace all of the beams in the superstructure.

Photo Credit: Ronald D. Jantzen

Figure 2. Photo. Bridge fascia immediately after fire.

PROJECT OBJECTIVE

The objective of this project is to determine if the July 12, 2005 incident on the U.S. Route 7 bridge over the Norwalk River caused a significant deterioration of the structural capacity of the bridge. The beams in the structure were numbered 1 through 15 beginning at the eastern fascia beam. Beams 3, 4, 7, and 14 were salvaged from the bridge and transported to the FHWA's Turner-Fairbank Highway Research Center. The condition of the concrete was investigated and full-scale tests were completed on the four beams to determine their remaining flexural capacity.

OVERVIEW OF REPORT

This report is divided into six chapters. Chapter 1 provides background information about the project. Chapter 2 details the experimental program that was implemented. Chapter 3 describes the material characterization testing that was completed. Chapter 4 details that flexural testing of the four box beams. Chapter 5 discusses the results that are presented in the earlier chapters. Chapter 6 presents a summary of the findings of this investigation.

CHAPTER 2. EXPERIMENTAL PROGRAM

INTRODUCTION

The primary emphasis of the test program was to determine the ultimate flexural capacity of the box beams in the bridge. The four beams came from different parts of the bridge and were likely subjected to varying levels of fire intensity. As such, the test matrix was designed to subject the four beams to identical loading conditions from test initiation through flexural failure. Prior to flexural testing the beams were visually surveyed for damage relating to the fire. After flexural testing, portions of the bottoms of the beams undamaged by the flexure tests were more thoroughly investigated through coring, visual inspection, and petrographic examination.

FLEXURE TEST SETUP AND INSTRUMENTATION

The setup for the flexure tests was designed to create a constant moment region at midspan of the beam. The beams were tested on a 14.1 m (46 ft 4 inches) span with two point loads applied 0.91 m (3 ft) on either side of midspan. The beams were supported at both ends by a 200-mm- (8-inch-) wide steel plate that rested on a roller bearing. The loads were applied to each beam through a 300-mm- (12-inch-) wide steel plate that spanned the width of the beam and was grouted to the top flange. Figure 3 is a photograph showing the test setup for the flexural loading of these box beams.

Figure 3. Photo. Flexural loading of a box beam.

The four beams had the same nominal midspan cross section as shown in Figure 4. The 0.64-m-(25-inch-) deep, 0.91-m- (36-inch-) wide box beams each contained two 0.305-m-(12-inch-) diameter circular voids located 0.32 m (12.5 inches) down from the top of the beam. The voids were formed with cardboard tubes that were capped at the quarter points and at midspan to allow for a continuous diaphragm across the bridge. Each beam was prestressed with thirty-six 9.5–mm- (0.375-inch-) diameter prestressing strands in the bottom flange, and two of these same strands in the top flange. Two number 4 rebars were also located in the top flange, serving to aid in installation of the mild steel reinforcement shear stirrups.

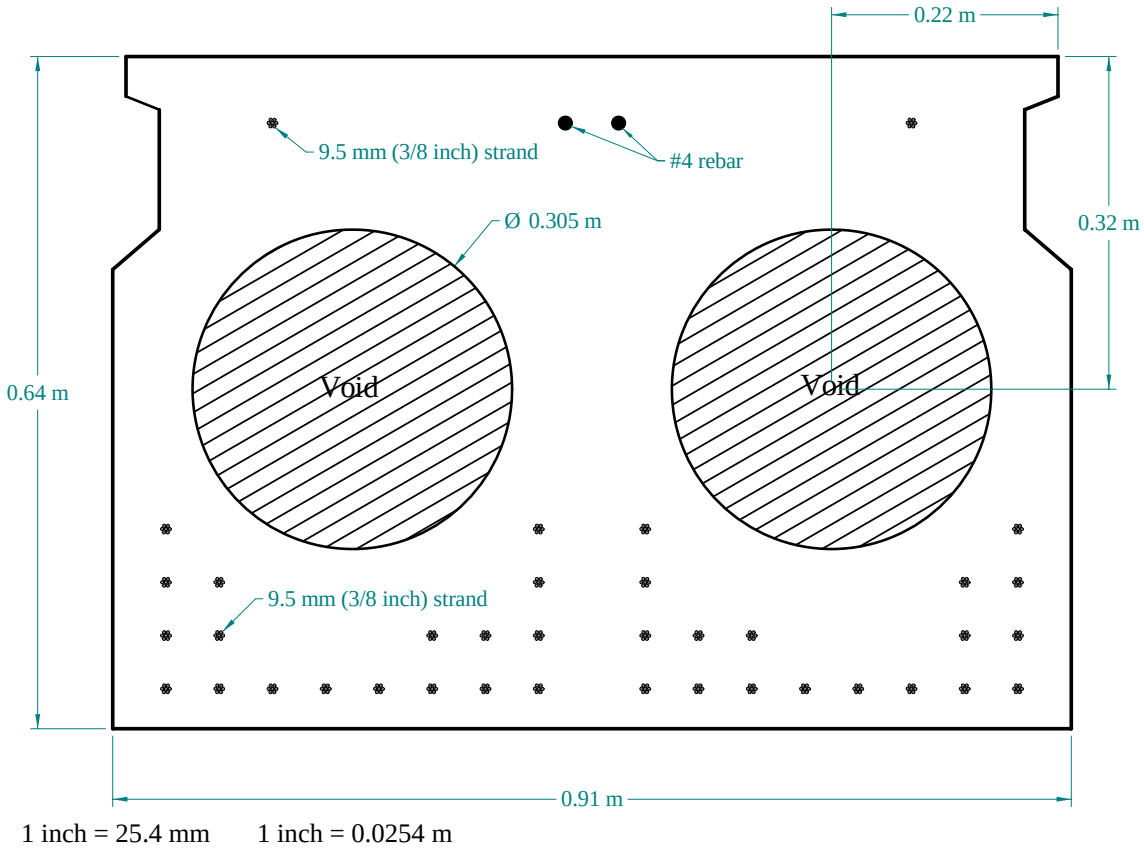

Figure 4. Illustration. Standard cross section of voided box beam.

After failure of each beam at the midspan cross section, this cross section was examined to determine as-built dimensions. It must be noted that the likely intended cross-sectional dimensions are shown in Figure 4, but that the actual as-built dimensions varied. For instance, the total minimum web thickness at middepth of the voids is 0.305 m (12 inches). At this location, the distance from a particular void to the outside face of the beam varied amongst the beams from a low of 51 mm (2 inches) in one beam to a high of 152 mm (6 inches) in another beam. Additionally, note that the distance from the bottom flange to the center of the bottom row of prestressing strands ranged from 38 to 51 mm (1.5 to 2.0 inches) throughout the beams.

The instrumentation plan implemented on each of the four tests included load cells, strain gages, and linear string potentiometers. Four load cells measured the load applied to the beam through

the pair of hydraulic jacks located at each of the two load points. Eleven resistance strain gages (120 ohm resistance, 51 mm- (2 inch-) gage length) were applied to the midspan cross section of each of the beams. Three of these gages were applied to the top of the beam, with one on the midline and the other two located symmetrically 330 mm (13 inches) from the midline. The other eight gages were affixed to the north and south elevations of the beam, with gages located 102, 203, 305, 406 mm (4, 8, 12, and 16 inches) down from the top of the beam on each face. All strain gages measured longitudinal strain in the beam. Finally, seven string potentiometers were attached to the midline of the bottom of each beam to measure vertical deflections. The potentiometers were placed at midspan and symmetrically about the midspan at 0.91, 2.74, and 4.57 m (3, 9, and 15 ft) east and west of midspan. These 22 instruments were read continuously throughout the test, and their readings were saved periodically at each load and/or displacement step.

CHAPTER 3. MATERIAL CHARACTERIZATION

INTRODUCTION

A series of investigations were completed to describe the characteristics of the concrete present in the four box beams. The first of these investigations focused on quantifying the compressive behaviors of the concrete. Second, a visual examination of the box beams was completed. Finally, a petrographic examination of the concrete was conducted.

CONCRETE MATERIAL PROPERTIES

After each beam failed under flexural loading, each end of each beam was cored to extract concrete samples. Three cores were extracted from each solid end-region of the eight beam halves. Approximately 254-mm- (10-inch-) long cores were initially drilled from the top of each beam. This region was lightly reinforced, thus no cores contained any embedded steel. In all cases, the cores each had a 102-mm (4-inch) diameter and were approximately 203 mm (8 inches) in length.

The compressive strength, modulus of elasticity, and density of the concrete contained in the four box beams was determined based on these cores and is shown in Table 1. The ends of the cores were prepared via grinding, then the length, diameter, and weight of the cores was determined. The density of the concrete was calculated based on these measurements. The density values shown in the table are based on the cores that were later tested in compression.

Table 1. Compressive strength, modulus of elasticity, and density.

Beam Number	Coring Site*	Density† (kg/m^3 (lb/ft^3))	Compressive Strength† (MPa (ksi))	Modulus of Elasticity‡ (GPa (ksi))
3	East	2,400 (150)	61 (8.9)	32.1 (4650)
3	West	2,400 (150)	66 (9.6)	35.9 (5210)
4	East	2,390 (149)	58 (8.4)	30.1 (4360)
4	West	2,410 (150)	67 (9.7)	35.2 (5100)
7	East	2,400 (150)	45 (6.6)	26.5 (3840)
7	West	2,400 (150)	52 (7.6)	27.0 (3910)
14	East	2,420 (151)	61 (8.9)	37.9 (5500)
14	West	2,440 (152)	64 (9.3)	35.4 (5140)

* East and West denote the end of the beam as oriented during laboratory structural testing.
† Two specimens were tested for each test site, and the average result is presented.
‡ One specimen was tested for each test site.
kg/m^3 = kilogram per cubic meter, lb/ft^3 = pound per cubic foot, MPa = megapascals, GPa = gigapascals

The ASTM C39 “Standard Test Method for Compressive Strength of Cylindrical Concrete Specimens” was followed for the compression testing of two cores from each coring site.[(1)] The average strength from these two tests is presented in Table 1. Note the relatively high

compressive strengths greater than 55 MPa (8 ksi) for beams 3, 4, and 14, while the compressive strength of beam 7 is slightly lower.

The ASTM C469 "Standard Test Method for Static Modulus of Elasticity and Poisson's Ratio of Concrete in Compression" was used to determine the modulus of elasticity of the concrete.[(2)] One core from each coring site was tested. Each core was loaded three times up to 40 percent of its anticipated compression strength, with the results from the second and third loadings being used to calculate the modulus of elasticity. The axial deformation of the core was captured through the use of a pair of parallel rings attached to the top and bottom of the cylinder, allowing for a gage length of 102 mm (4 inches) between rings. The distance between the rings was measured through the use of three linear variable differential transformers (LVDTs). The LVDTs and load readings were all electronically captured throughout the testing via a data acquisition system.

Subsequent to the completion of the ASTM C469 testing on one core from each end of each beam, the same cores were tested to failure. In these tests, the ASTM C469 measurements were again captured, but the loading was not halted at 40 percent of the anticipated peak compressive load. These tests provided an indication of the full compressive stress-strain response of the concrete in the beams and specifically the strain levels exhibited by the concrete as it approached compressive failure. Figure 5 shows a representative response from one of the cores. Of the eight cores tested, the average compressive strain observed at the peak compressive stress was 0.00275 with a standard deviation of 0.00018.

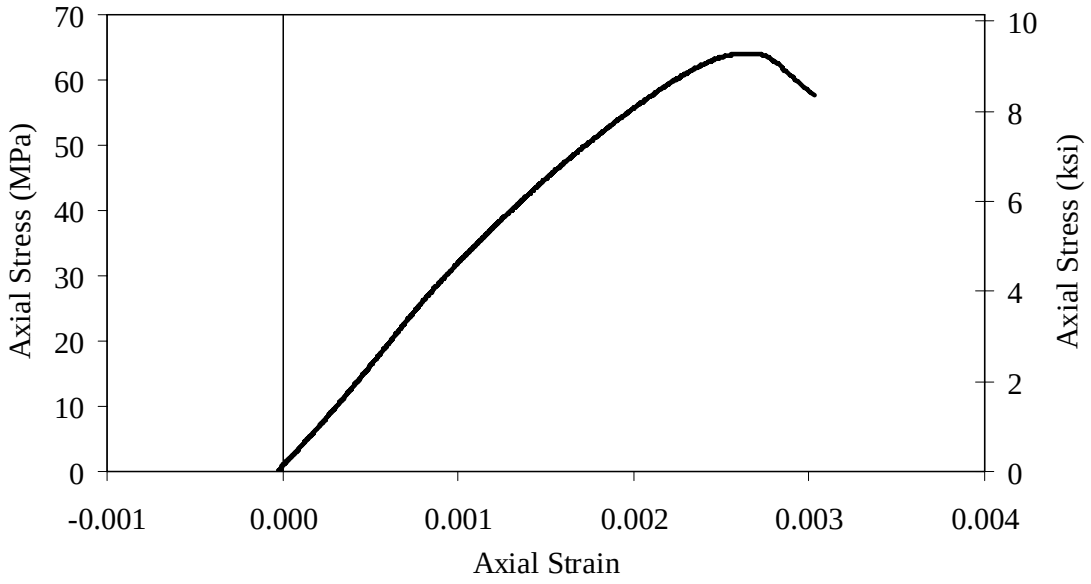

Figure 5. Graph. Compressive stress-strain behavior of core from Beam 3.

VISUAL EXAMINATION OF FIRE-DAMAGED CONCRETE

A visual examination was completed on the exterior surfaces of the four fire-damaged beams that were tested in flexure. Recall that these four beams were all interior beams within an adjacent

box-beam bridge that was covered by a thick asphalt overlay. As such, these beams only exhibited fire related damage on their bottom surfaces. Figure 6 shows the damage on the bottom surface of Beam 4. As a whole, the bottom surfaces of Beams 3, 4, and 7 exhibited similar damage with large patches of scaled concrete. Beam 14 exhibited more widespread surface scaling with most of the bottom flange being uniformly scaled. In all cases, the scaling was focused more toward the middle of the bottom flange, with the bottom flange edges along the length of the beams remaining primarily intact. In general throughout the four beams, the average scaling depth was approximately 10 mm (0.4 inch) with some local scaling of up to 15 mm (0.6 inch) deep. Based on a limited number of scaled but still intact scaled areas, the scaling seems to have occurred in small, thin sheets passing through the aggregate. Fractured aggregate is also visible on a significant portion of the scaled areas, also indicating that the scaling occurred through the aggregate.

Figure 6. Photo. Bottom face of Beam 4.

PETROGRAPHIC EXAMINATION OF FIRE-DAMAGED CONCRETE

Petrographic examinations were completed on two cores from Beam 4.[(3)] In each case, 95-mm-(3.75-inch-) diameter cores approximately 152 mm (6 inches) long were extracted from the center of the bottom flange of the beam. One core was extracted from the west quarterpoint and one was extracted from the east quarterpoint along the length of the span.

The petrographic examinations were completed in accordance with ASTM C856 “Standard Practice for Petrographic Examination of Hardened Concrete.”[(4)] The investigation included the examination of thin section samples taken from six depths along the length of each core, as well as polished surface samples covering the length of each core.

This concrete was determined to include an angular crushed diabase coarse aggregate with a maximum size of approximately 25 mm (1 inch), a primarily quartz fine aggregate from natural sand, and a reasonably well-hydrated cement paste. The concrete appears to be air entrained with small spherical air voids. The small amount of entrapped air indicates that the concrete in these cores was well consolidated.

The petrographic examination determined that the concrete in the cores suffered damage to a depth of approximately 25 mm (1 inch) from the exposed surface. In this zone the concrete exhibits both small and large size cracks extending through the paste, through the aggregate, and along the paste aggregate interface. These cracks tend to be perpendicular to the exposed surface of the core. It is likely that these cracks occurred due to desiccation-related shrinkage of the concrete caused by the fire. Concrete beyond the 25 mm (1 inch) zone exhibits much less severe damage with fewer cracks and smaller crack sizes. Figure 7 presents a photomicrograph with a 4.0-mm- (0.157-inch-) width of field and with the center of the photograph located 10 mm (0.4 inch) from the exposed surface of the core to the right of the photo. This figure shows a large crack extending through the 25-mm-(1-inch-) deep zone of damage.

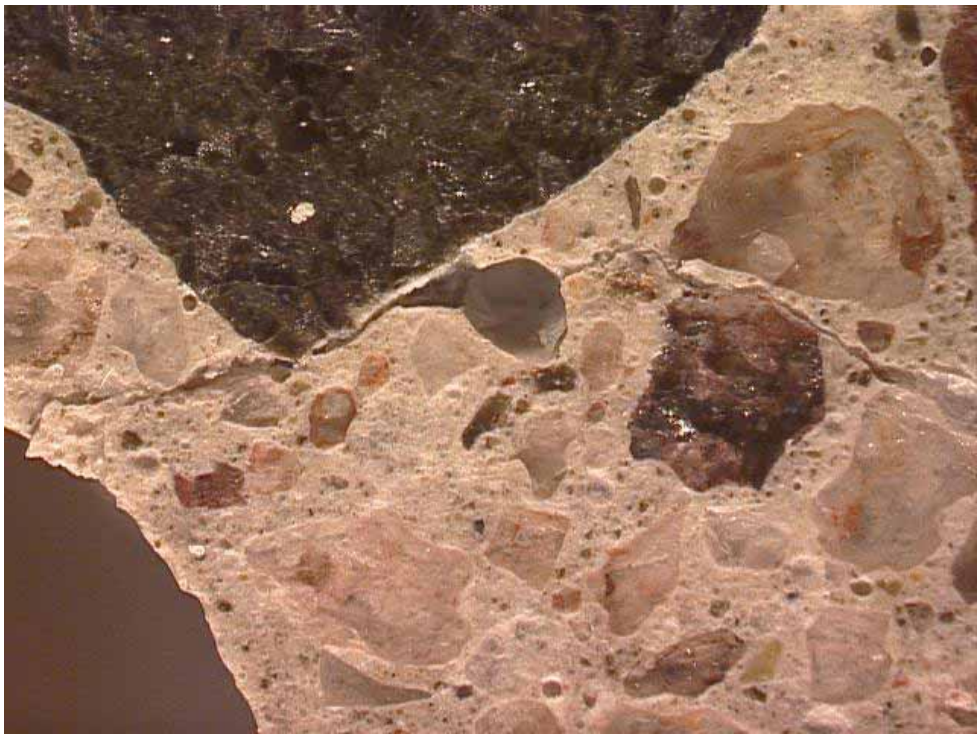

Figure 7. Photo. Photomicrograph of a crack near the exposed surface of the concrete.

CHAPTER 4. BOX BEAM FLEXURE TESTING

INTRODUCTION

Four 0.64 m (25 inch) deep box beams were loaded in four-point bending to determine their flexural behavior. Beams 3, 4, 7, and 14 were loaded under identical conditions in order to capture any deviations in behavior exhibited by the beams. The results of these tests are described below.

TEST PROCEDURE

The tests were conducted to determine the static flexural capacity of the four beams. Recall that all beams were loaded on a 14.1-m (46-ft 4-inch) span with two point loads applied 0.91 m (3 ft) on either side of midspan. Initially, the applied load was increased in 3-kip increments. After flexural cracking was observed in the bottom flange, the loading increment was revised to instead focus on midspan vertical displacement increments. The displacement was incremented by 2.5 mm (0.1 inch) thereafter until flexural failure of the beam.

During the test, the incremental increase of applied load and midspan deflection was periodically halted to allow for the capture of the residual flexural stiffness of the beam. The capture of the residual stiffness was completed at least four times for each beam, occurring at applied load levels of approximately 178, 289, 356, and 400 kN (40, 65, 80, and 90 kips). In general, this process included releasing the load to 80 percent of the peak load previously achieved and then reloading the beam in approximately 10 kN (2.2 kip) increments back to the peak load.

During the test, the loading was also periodically halted to map the flexural cracking apparent on the north and south faces of each beam. Cracks apparent prior to the start of the test, whether due to stresses imparted during handling and transportation of the beams at the bridge site or due to other forces, were marked prior to the start of the test.

BEAM 3

The flexural behavior of Beam 3 was captured through the implementation of the test procedure described above. Figure 8 shows the total applied load versus midspan vertical deflection plot. As is shown on this figure, the beam behaved in an elastic manner until approximately 245 kN (55 kips) of load was applied. This corresponds to an applied moment of 751 kN-m (554 kip-ft). The beam then exhibited decreasing flexural stiffness as the load increased up to 463 kN (104 kips). Flexural failure of the beam occurred at this load when the midspan deflection was 343 mm (13.5 inches). This applied load corresponds to an applied moment of 1,421 kN-m (1,048 kip-ft). Figure 9 shows the deflected shape of the beam at incrementally higher load levels throughout the test.

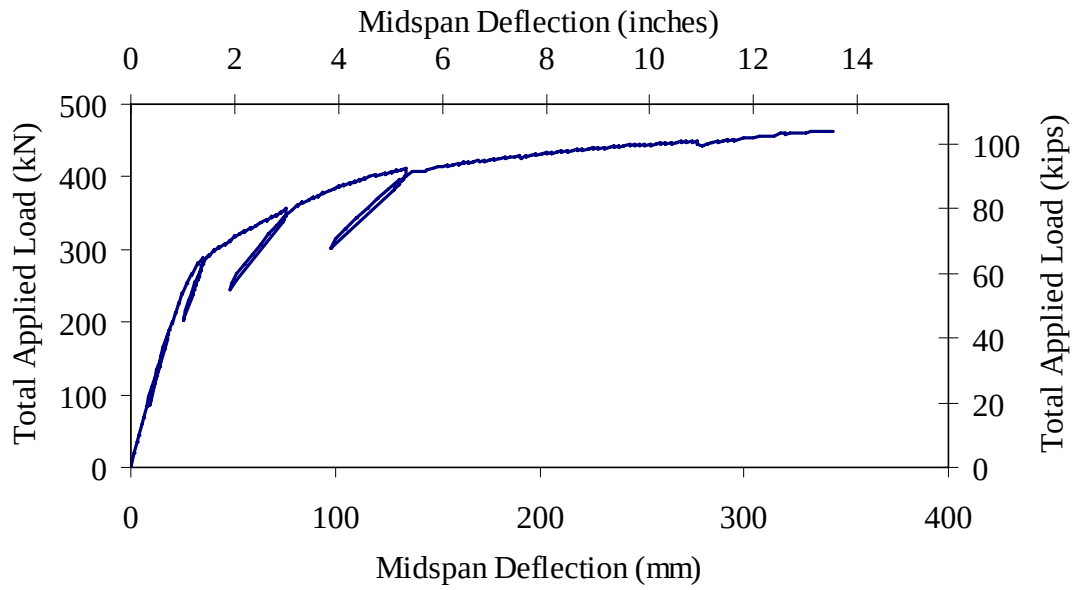

Figure 8. Graph. Applied load versus midspan vertical deflection for Beam 3.

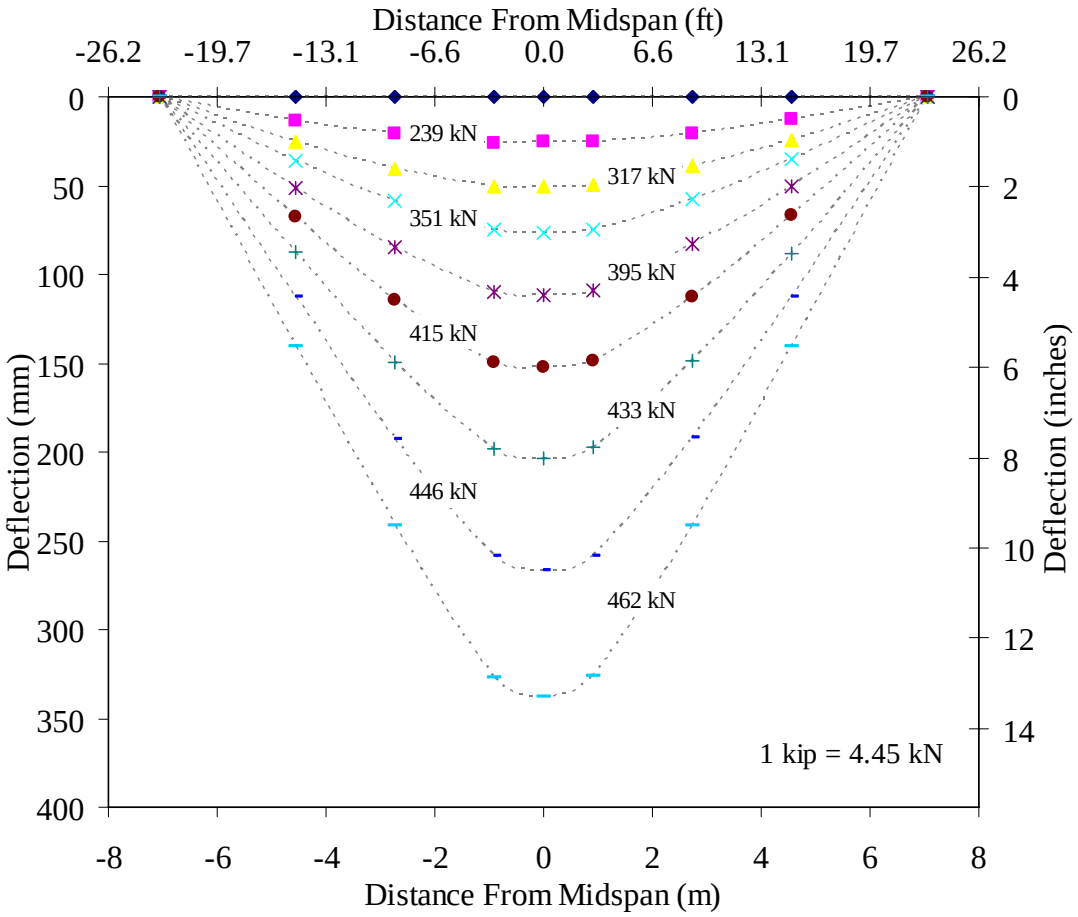

Figure 9. Graph. Deflected shape of Beam 3.

Figure 10 plots the midspan neutral axis depth from the top of the beam versus the load applied to the beam. The neutral axis depth is calculated for each face of the beam based on the operational strain gages providing reliable readings at a given load level. The neutral axis depths from each face were then averaged to determine the depth plotted in the figure. As would be expected, after the beam began exhibiting inelastic behaviors (i.e., concrete cracking), the neutral axis began to rise.

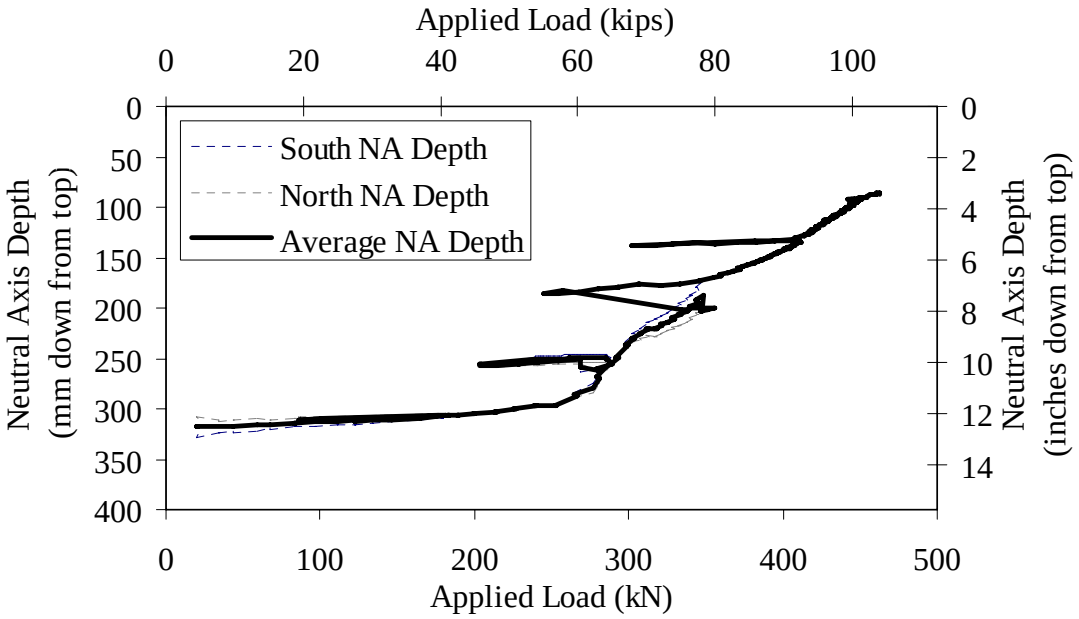

Figure 10. Graph. Midspan neutral axis depth from top of Beam 3.

The failure of this beam, although preceded by significant tensile cracking of the bottom flange and a significant rise in the neutral axis, was caused by a compression failure of the concrete in the top flange. Figure 11 provides a photograph showing the sudden nature of the final failure. No spalling of concrete or rupturing of strands occurred prior to the compression failure of the top flange.

BEAM 4

Beam 4 was tested in a similar fashion to Beam 3, described above. Figure 12 shows the total applied load versus midspan vertical deflection plot. As is shown on this figure, the beam behaved in an elastic manner until approximately 245 kN (55 kips) of load was applied. This corresponds to an applied moment of 751 kN-m (554 kip-ft). The beam then exhibited decreasing flexural stiffness as the load increased up to 458 kN (103 kips). Flexural failure of the beam occurred at this load when the midspan deflection was 284 mm (11.2 inches). This applied load corresponds to an applied moment of 1,407 kN-m (1,038 kip-ft). Figure 13 shows the deflected shape of the beam at incrementally higher load levels throughout the test.

Figure 14 plots the midspan neutral axis depth from the top of the beam versus the load applied to the beam. As with Beam 3, after the beam began exhibiting inelastic behaviors (i.e., concrete cracking), the neutral axis began to rise.

Figure 11. Photo. Failure of Beam 3.

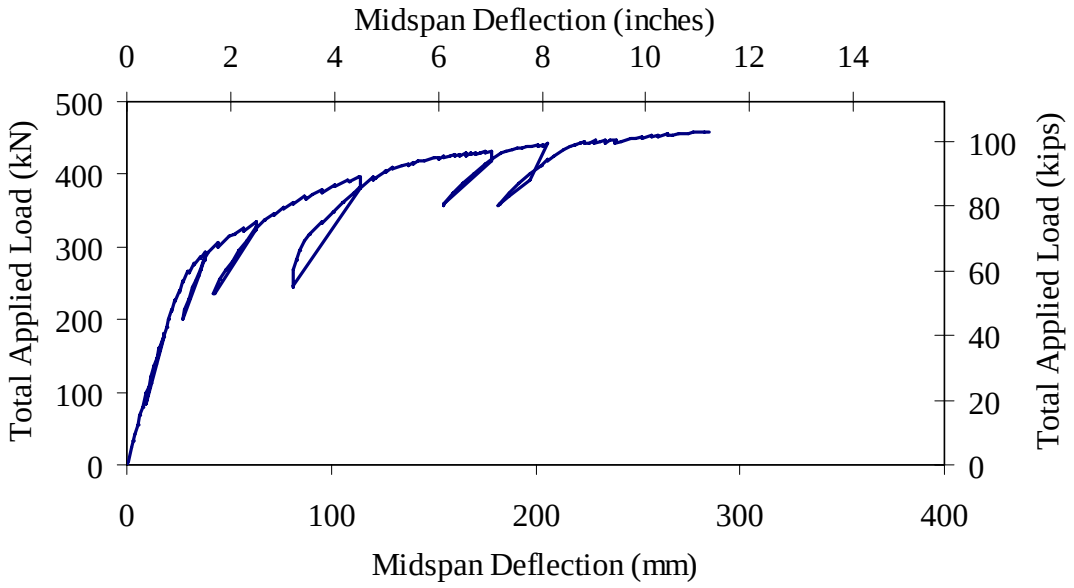

Figure 12. Graph. Applied load versus midspan vertical deflection for Beam 4.

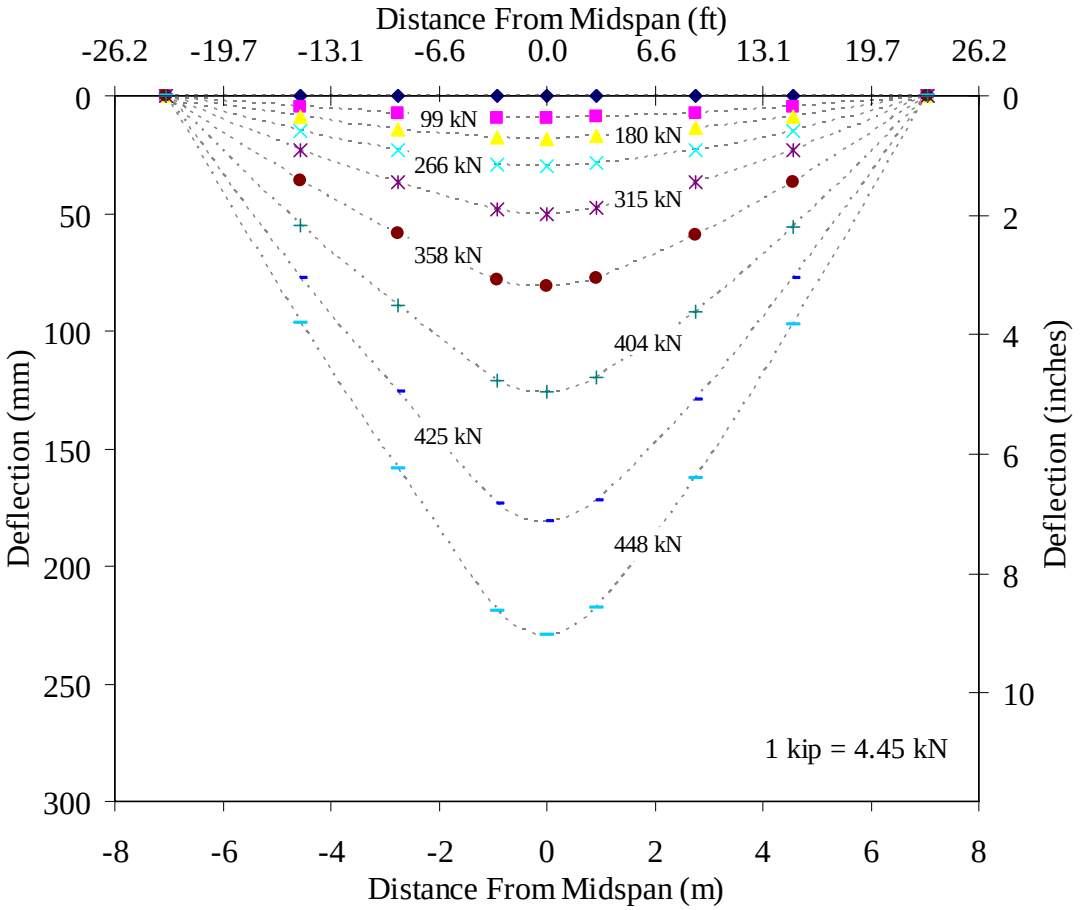

Figure 13. Graph. Deflected shape of Beam 4.

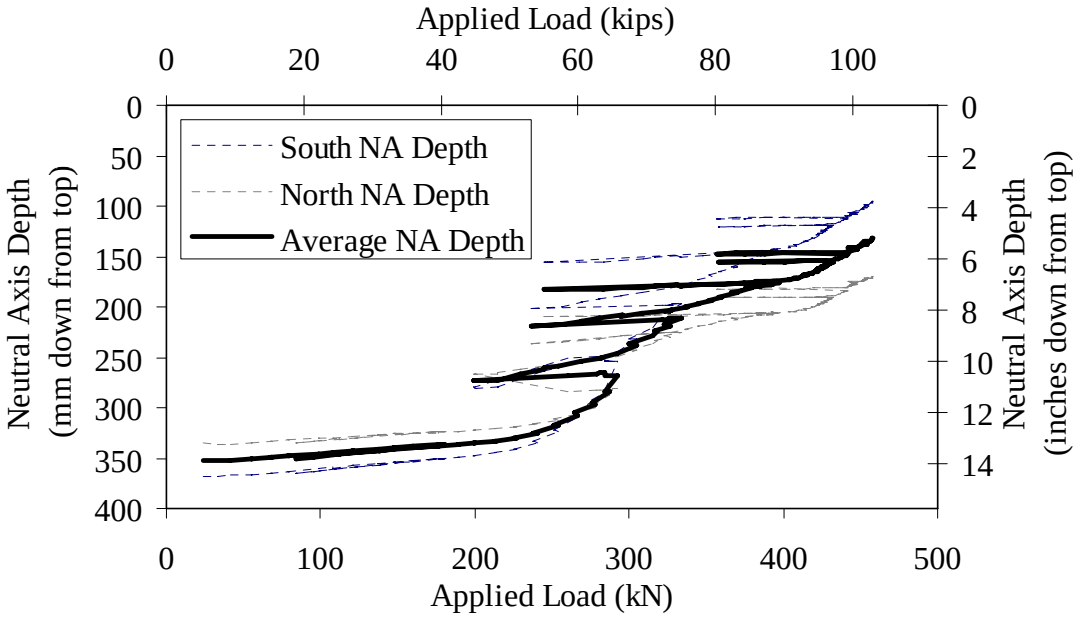

Figure 14. Graph. Midspan neutral axis depth from top of Beam 4.

Figure 15 provides a photo of the deflected shape of the beam at the maximum applied load. Clearly, this beam exhibited significant deflection capacity prior to failure. The failure of this beam, although preceded by significant tensile cracking of the bottom flange and a significant rise in the neutral axis, occurred in a brittle manner, likely as a result of the compression failure of the concrete. Figure 16 provides a photograph of the beam just after failure. No spalling of concrete or rupturing of strands occurred prior to failure of the beam.

Figure 15. Photo. Deflection of Beam 4 at maximum applied load.

BEAM 7

Beam 7 was tested in a similar fashion to Beams 3 and 4, described above. Figure 17 shows the total applied load versus midspan vertical deflection plot. As is shown on this figure, the beam behaved in an elastic manner until approximately 223 kN (50 kips) of load was applied. This corresponds to an applied moment of 681 kN-m (503 kip-ft). The beam then exhibited decreasing flexural stiffness as the load increased up to 445 kN (100 kips). Flexural failure of the beam occurred at this load when the midspan deflection was 236 mm (9.3 inches). This applied load corresponds to an applied moment of 1,362 kN-m (1,005 kip-ft). Figure 18 shows the deflected shape of the beam at incrementally higher load levels throughout the test.

Figure 19 plots the midspan neutral axis depth from the top of the beam versus the load applied to the beam. As with Beams 3 and 4, after the beam began exhibiting inelastic behaviors (i.e., concrete cracking), the neutral axis exhibited a marked decrease in depth from the top flange.

The failure of this beam, although preceded by significant tensile cracking of the bottom flange and a significant rise in the neutral axis, occurred in a brittle manner as a result of the compression failure of the concrete. Figure 20 provides a photograph captured during failure of the beam. No spalling of concrete or rupturing of strands occurred prior to failure of the beam.

Figure 16. Photo. Failed Beam 4.

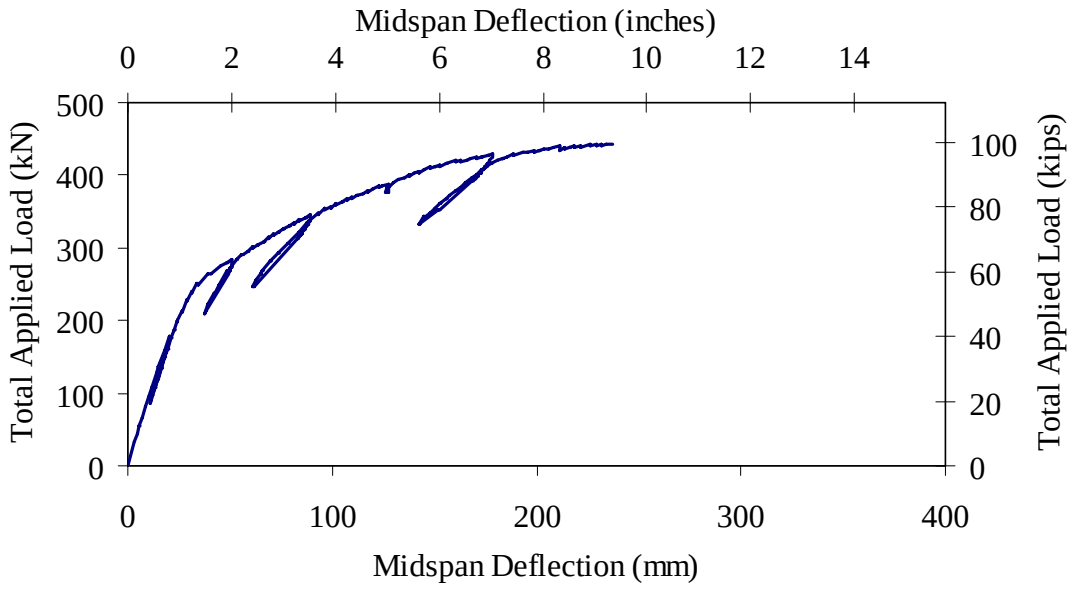

Figure 17. Graph. Applied load versus midspan vertical deflection for Beam 7.

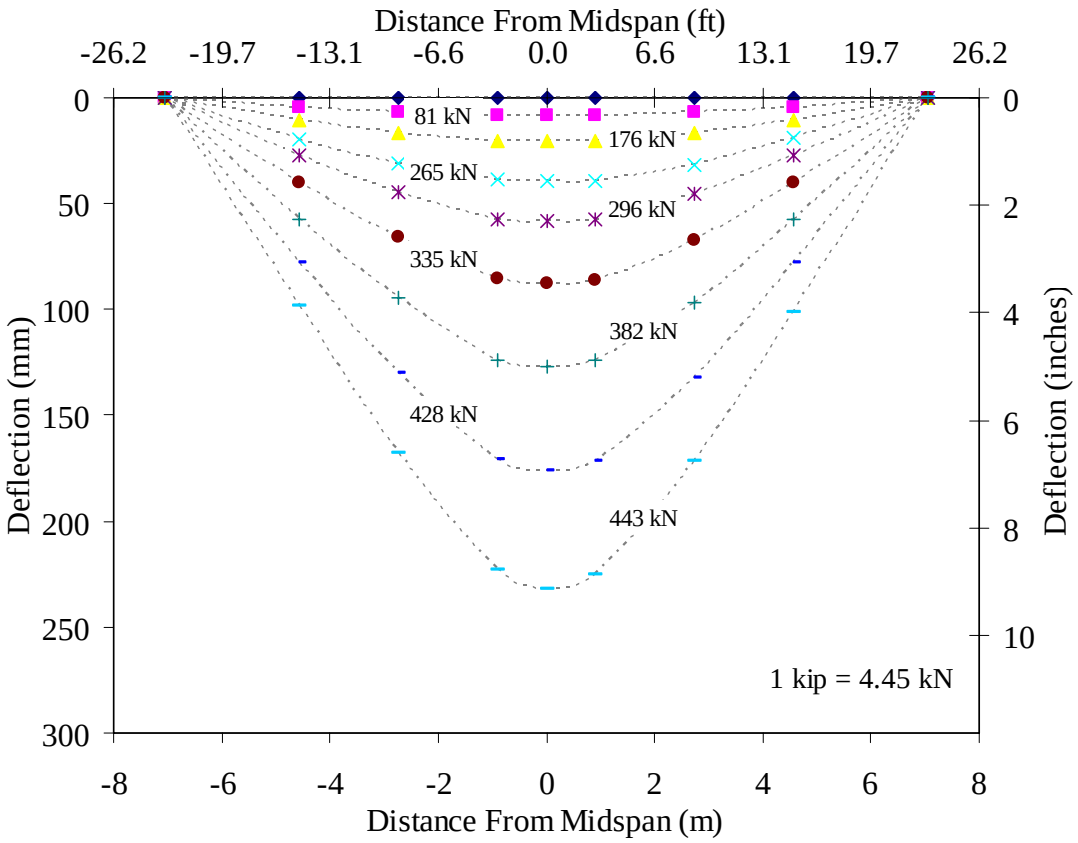

Figure 18. Graph. Deflected shape of Beam 7.

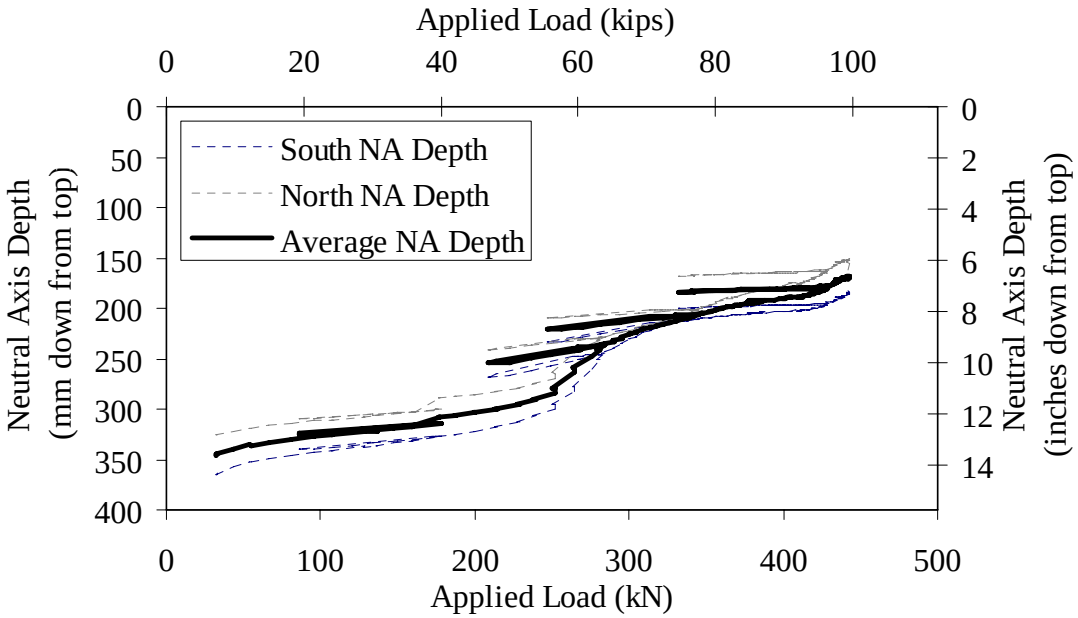

Figure 19. Graph. Midspan neutral axis depth from top of Beam 7.

Figure 20. Photo. Failure of Beam 7.

BEAM 14

Beam 14 was tested in a similar fashion to the previously discussed beams. Figure 21 shows the total applied load versus midspan vertical deflection plot. As is shown on this figure, the beam behaved in an elastic manner until approximately 223 kN (50 kips) of load was applied. This corresponds to an applied moment of 681 kN-m (503 kip-ft). The beam then exhibited decreasing flexural stiffness as the load increased up to 423 kN (95 kips). Flexural failure of the beam occurred at this load when the midspan deflection was 236 mm (9.3 inches). This applied load corresponds to an applied moment of 1,301 kN-m (960 kip-ft). Figure 22 shows the deflected shape of the beam at incrementally higher load levels throughout the test.

Figure 23 plots the midspan neutral axis depth from the top of the beam versus the load applied to the beam. As with the previously discussed beam tests, after the beam began exhibiting inelastic behaviors (i.e., concrete cracking), the neutral axis exhibited a marked decrease in depth from the top flange.

The failure of this beam, although preceded by significant tensile cracking of the bottom flange and a significant rise in the neutral axis, occurred in a brittle manner likely as a result of compression failure of the concrete in the top flange. Figure 24 provides a photograph captured just after failure of the beam. No spalling of concrete or rupturing of strands occurred prior to failure of the beam.

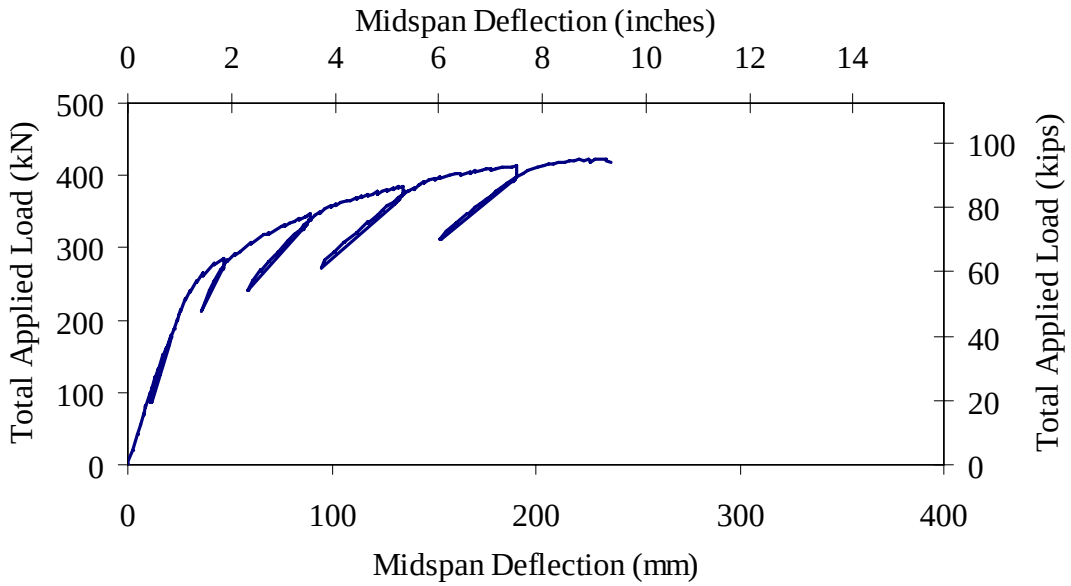

Figure 21. Graph. Applied load versus midspan vertical deflection for Beam 14.

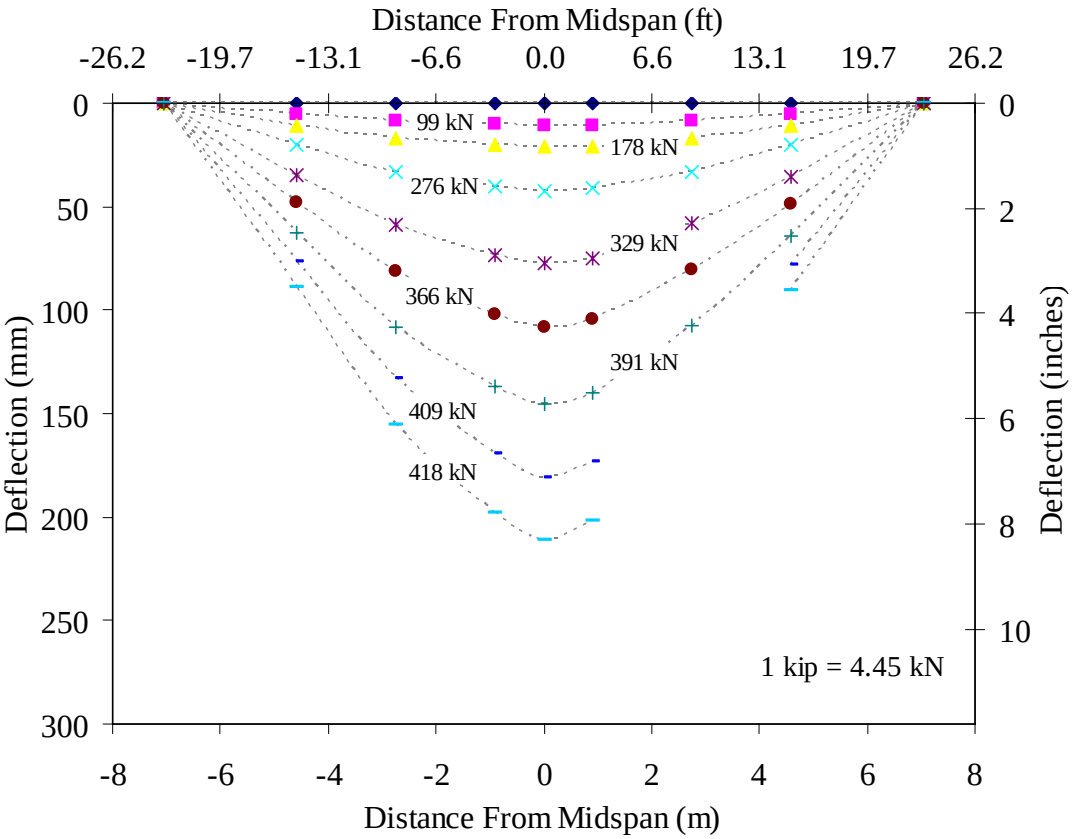

Figure 22. Graph. Deflected shape of Beam 14.

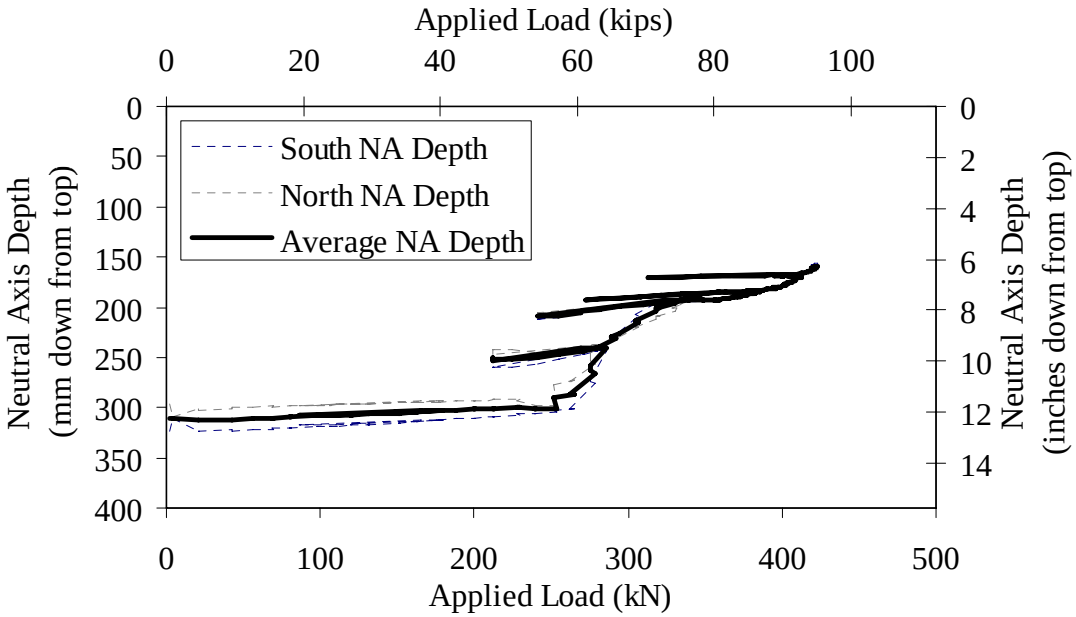

Figure 23. Graph. Midspan neutral axis depth from top of Beam 14.

Figure 24. Photo. Failed Beam 14.

COMBINED FLEXURE RESULTS

The flexural testing of these four beams under identical loading configurations allows for direct comparisons between observed behaviors. In terms of applied flexural capacity, the four beams behaved similarly. Beam 14 exhibited the lowest capacity at 1,301 kN-m (960 kip-ft), while Beam 3 exhibited the highest capacity at 1,421 kN-m (1,048 kip-ft). Under this loading arrangement, the midspan moment caused by the beam self-weight is 271 kN-m (200 kip-ft). Thus, the ultimate moment capacity of these beams was at least 1,572 kN-m (1,160 kip-ft).

The live load moment capacities of each of these interior beams in service can be calculated by subtracting the inservice dead load moments from the experimentally determined ultimate moment capacity. Recalling that these beams carried an asphalt wearing surface in field that was not present during the laboratory tests, the ultimate live load moment capacity of each of the interior beams (assuming no dead load distribution between beams in the bridge and using the actual dead loads) was calculated to be at least 1206 kN-m (890 kip-ft).

In general, all four beams exhibited elastic behavior through approximately 610 kN-m (450 kip-ft) of applied moment. Thus, the total moment on the midspan cross section at the cessation of elastic behavior was approximately 881 kN-m (650 kip-ft). In terms of live load moment capacity, 515 kN-m (380 kip-ft) of moment could be applied to a beam prior to the initiation of inelastic behavior.

The experimentally observed midspan deflection at flexural failure was also similar, with all four beams failing after at least 230 mm (9 inches) of deflection had occurred. Figure 25 shows the backbone curves for the applied load versus midspan deflection behavior of the four beams. The figure clearly shows that all four beams exhibited ductile behavior with significant deflection occurring prior to flexural failure.

The midspan compression flange strain throughout the loading of the beam is also instructive with regard to the flexural behavior. The prestress and dead load moments resisted by the beam at midspan combine to create a compressive strain of approximately 0.0001 in the top flange. Figure 26 plots the average strain observed in the three gages on the top flange versus the moment that was applied to the midspan cross section. As in Figure 25, this figure only presents the backbone of the response with the unloading-reloading sequences having been eliminated from the data set. Adding the initial strain in the top flange of the beam to the applied strain values shown in Figure 26 results in the determination that the flexural failures of the beams occurred when the compressive strain in the top flange was between 0.0021 and 0.0028. Recall that the flexural failures of two of these beams were observed to be caused by compression failure of the top flange concrete, and the failure of the other two may have been caused by the same mechanism. Given the widely used concrete flexural design assumption wherein concrete is assumed to fail in compression at a strain of 0.003, the failure of these beams at compression flange strains below 0.0028 is notable.

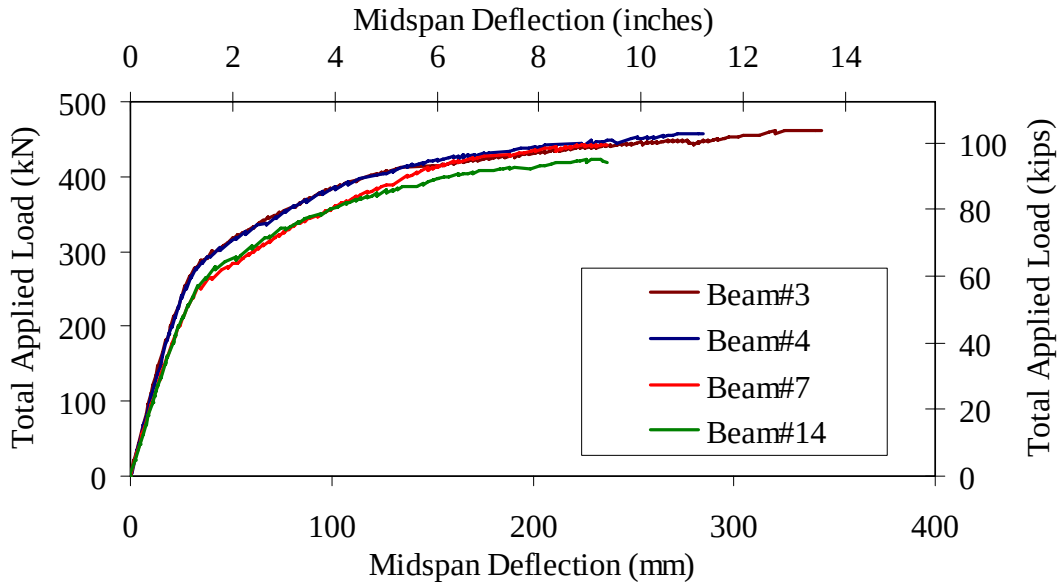

Figure 25. Graph. Applied load versus midspan vertical deflection backbone curves.

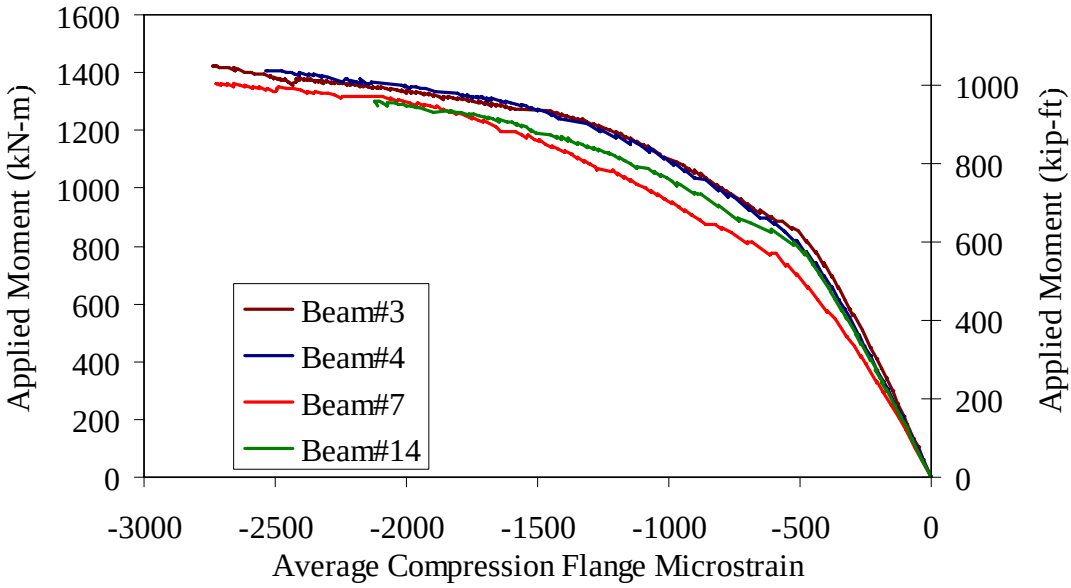

Figure 26. Graph. Applied moment versus average compression flange strain backbone curve.

CHAPTER 5. DISCUSSION OF RESULTS

The objective of this project was to determine if the incident on the Route 7 bridge had significantly degraded the flexural capacity of the adjacent box beams. The full scale flexural testing of four of these beams indicates that the live load elastic flexural capacity is approximately 515 kN-m (380 kip-ft). The same tests indicated that the live load ultimate flexural capacity is at least 1,206 kN-m (890 kip-ft). In terms of total load, the experimentally determined ultimate flexural capacity of these beams was determined to be at least 1,572 kN-m (1,160 kip-ft). For comparison, the analytically determined ultimate flexural capacity of these beams prior to the incident was 1,407 kN-m (1,038 kip-ft).

Although the four beams were originally located in different parts of the bridge, the large-scale test results and the visual examination of the bridge indicate that all the beams likely underwent a similar level of degradation during the incident. Given that the weakest of the four beams carried an ultimate flexural capacity that was more than 10 percent greater than the pre-incident analytically determined ultimate flexural capacity, it seems that the beams were not significantly structurally degraded by the fire.

However, the incident may have caused sufficient damage to the tensile-region concrete in these beams to impair their long-term flexural behavior. The as-built concrete cover below the midspan cross-section bottom row of strands varies between 33 and 46 mm (1.3 and 1.8 inches). Recall that the fire caused surface spalling on the bottom flange of the beams in many areas to a depth of 10 mm (0.4 inch), and the petrographic examination indicated that an additional 25 mm (1 inch) of intact concrete exhibits penetrating cracks caused by the fire. Combined, these facts seem to indicate that the bottom row of strands may have had decreased long-term protection from corrosive forces.

CHAPTER 6. SUMMARY

A fiery incident involving a gasoline tanker truck caused significant damage to an adjacent member box-beam bridge in southwestern Connecticut. Although ConnDOT decided to replace the superstructure of the bridge, there was a question as to whether the type of damage that these box beams experienced was sufficient to critically impair the structure's ability to serve its intended purpose. To answer this question, ConnDOT coordinated with the FHWA's Turner-Fairbank Highway Research Center to investigate the remaining flexural capacity of the beams in the bridge.

Four of the beams from the bridge were loaded in flexure to failure. These tests indicated that each of the beams retained sufficient flexural capacity to resist an 881 kN-m (650 kip-ft) moment while remaining elastic and to resist a 1,572 kN-m (1,160 kip-ft) moment prior to ultimate flexural failure. This ultimate value is greater than the rated ultimate flexural capacity of each beam. As such, it seems that these beams had sufficient remaining flexural capacity to serve their intended purpose in the immediate aftermath of the fire.

The long-term viability of these beams is more questionable. The visual and petrographic examinations indicated that the damage to the bottom flange concrete was sufficient to allow pathways through the concrete to the depth of the bottom strands. Thus, it is possible that the bottom flange concrete would have experienced accelerated deterioration, leading to accelerated deterioration of the bottom row of strands and a long-term decrease in the flexural capacity of each beam.

REFERENCES

1. ASTM C39, "Standard Test Method for Compressive Strength of Cylindrical Concrete Specimens," American Society for Testing and Materials Standard Practice C39, Philadelphia, PA, 2005.

2. ASTM C469, "Standard Test Method for Static Modulus of Elasticity and Poisson's Ratio of Concrete in Compression," American Society for Testing and Materials Standard Practice C469, Philadelphia, PA, 2002.

3. Liu, R., *Petrographic Examination of Concrete Cores from a Fire Damaged Bridge in Connecticut*, Turner-Fairbank Highway Research Center Internal Report, July 2006, 11 pp.

4. ASTM C856, "Standard Practice for Petrographic Examination of Hardened Concrete," American Society for Testing and Materials Standard Practice C856, Philadelphia, PA, 2004.

HRDI-06/02-07(WEB)E